A Plasma Shape Identification with Magnetic Analysis for the Real-time Control on QUEST

Hasegawa, Makoto
Research Institute for Applied Mechanics, Kyushu University

Nakamura, Kazuo
Research Institute for Applied Mechanics, Kyushu University

Tokunaga, Kazutoshi
Research Institute for Applied Mechanics, Kyushu University

Zushi, Hideki
Research Institute for Applied Mechanics, Kyushu University

他

出版情報：電気学会論文誌Ａ（基礎・材料・共通部門誌）. 132 (7), pp.477-484, 2012-07-01. 電気学会
バージョン：

電気学会論文誌 A（基礎・材料・共通部門誌）
IEEJ Transactions on Fundamentals and Materials
Vol.132 No.7 pp.477-484 DOI: 10.1541/ieejfms.132.477

Paper

A Plasma Shape Identification with Magnetic Analysis for the Real-time Control on QUEST

Makoto Hasegawa*a) Non-member, Kazuo Nakamura* Member
Kazutoshi Tokunaga* Non-member, Hideki Zushi* Non-member
Kazuaki Hanada* Member, Akihide Fujisawa* Non-member
Hiroshi Idei* Non-member, Shoji Kawasaki* Non-member
Hisatoshi Nakashima* Non-member, Aki Higashijima* Non-member

(Manuscript received Oct. 28, 2011, revised March 14, 2012)

In order to identify plasma shape, there is a way to represent the plasma current profile with several parameters, and adjust these parameters with least-square technique in order for calculated magnetic values to accord with measured ones. Here, the plasma shape parameters such as minor radius, elongation, and triangularity are chosen as the fitting parameters to represent plasma shape more directly, and the applicability to the control of the plasma shape are described by evaluating its calculation time. In order to find minimum of an objective function with least-square technique, two methods are compared, namely a linear approximation method and a downhill simplex method. While high accuracies of the measured magnetic signals are required, the good reproducibility is obtained, and the plasma shape identification can be done within several milliseconds in both methods.

Keywords : plasma shape, eddy currents, downhill simplex method, real-time, QUEST

1. Introduction

In spherical tokamaks (STs), non-inductive current start-up experiments are executed[1)-4)] with interests toward the achievement of central solenoidless plasma operation. In this operation, the information of the plasma current shape is important, and has to be identified in real-time to control plasma shape. In some tokamaks, plasma shape control has been achieved by using real-time equilibrium reconstruction such as rtEFIT[5)-7)], where Grad-Shafranov equation is solved on the inside of last closed flux surface (LCFS). On the other hand, in non-inductive current start-up experiments, toroidal current not only inside but outside of LCFS is suggested to have a key role[2)]. In order to reconstruct plasma shape taking into account toroidal current outside of LCFS, several attempts are tested. One is equilibrium reconstruction which expands calculating area to the outside of LCFS[8)], and another is identification of plasma current shape by adjusting plasma shape parameters in order for calculated magnetic signals to accord with mesuared ones of magnetic probe and/or flux loops. From the view point of real-time identification of plasma shape, the latter is more suitable because of light calculation amount. In the CDX-U, the finite element description is used to represent the plasma current profile[9)]. On the other hand, in the LATE, the plasma current profile is represented by seven parameters which are the center position (R, z), 4 axis lengths of elliptic arcs, and a peaking factor[10)]. These two methods adjust the parameters by using a least square method. In the latter method, though it takes one second to calculate one profile, these methods don't refer to the possibility to use calculation results for the real-time control. Furthermore, it is considered to be more adequate to use plasma shape parameters such as minor radius, elongation, and triangularity for the representation of the plasma shape. In this paper, we propose the use of plasma shape parameters as the fitting parameters, and describe the applicability to the real-time calculation.

a) Correspondence to: Makoto Hasegawa.
E-mail: hasegawa@triam.kyushu-u.ac.jp
* Research Institute for Applied Mechanics, Kyushu University
6-1, Kasuga-koen, Kasuga, Fukuoka 816-8580, Japan

2. QUEST Device and Estimation Model

2.1 Plasma Control System Plasma Control Workstation (WS) controls peripheral systems of QUEST. The WS sends command signals to two RF systems (8.2 GHz, 200 kW), and one RF system (2.45 GHz, 50 kW). The WS also controls seven coil power supplies. The two power supplies are controlled by current command signals sent from the WS, and the others are controlled by the PID (Proportional Integral Derivative) control loops against power supply currents, sending current signals to the WS, and receiving voltage command signals. The WS is composed of PXI systems of the National Instruments Corporation, which contains the real-time OS based controller module (2.26 GHz Intel Core 2 Quad processor, 2 GBytes memory), one DIO module (16 ch digital input and output), and 6 FPGA (Field-Programmable Gate Array) modules (8 channel analog input and output). In the controller module, process threads are executed in parallel. One is a transaction thread for the data communication between the FPGA, DIO modules and the memory of the controller module. Another is a main thread which calculates physical quantities from raw voltage signals, and determines command signals according to the preprogrammed values or the response of plasma. These two threads are executed in 4 kHz frequency with the usage of two out of four cores. Figure 1 shows the poloidal cross section of QUEST. The WS

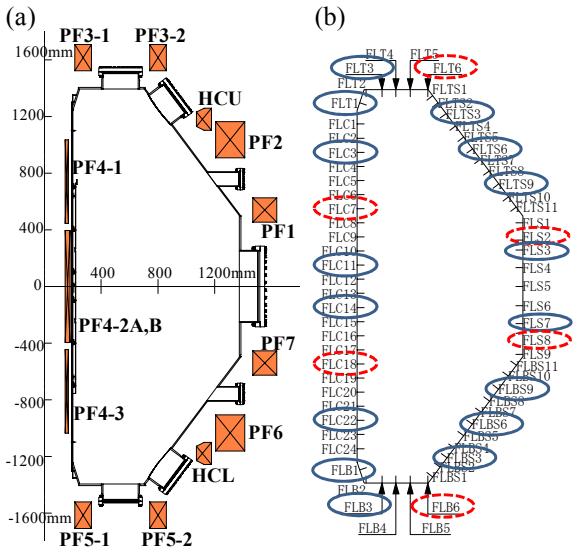

Fig. 1. The poloidal cross section of QUEST: (a) Positions of PF coils, (b) Installed positions of flux loops; The signals of the 22 encircled flux loops are acquired by WS. The flux loops encircled with dashed line are used to calculate plasma position

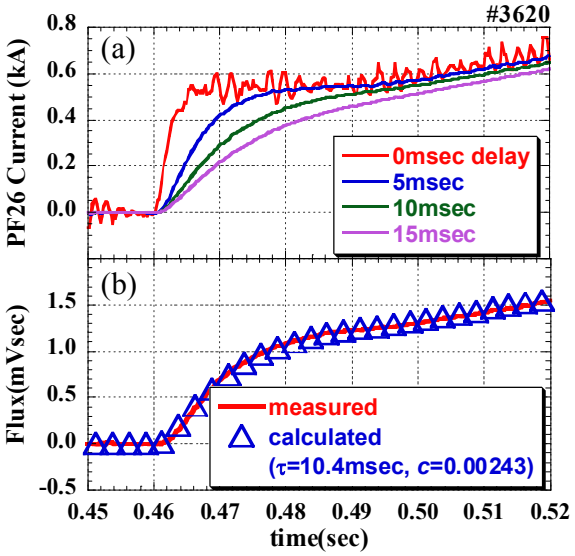

Fig. 2. Effect of eddy currents: (a) The PF26 coil current, and its calculated time-delayed wave forms, (b) The measured magnetic flux, and the time-delayed wave form of the PF26 coil current

acquires 22 flux loop signals out of 67 flux loops in order to determine the plasma position and its shape. To control the plasma vertical position, the HCU and HCL coils, which are connected oppositely, are used to make horizontal magnetic fields. The PF1 and PF7 coils (PF17) are connected serially. The PF2 and PF6 coils (PF26) are also connected serially to make vertical magnetic fields.

2.2 Eddy Current Removal The measured magnetic fluxes contain the components induced by plasma, PF coils, and eddy currents. In order to calculate the plasma position and its shape, the plasma-induced magnetic fluxes have to be extracted from the measured magnetic fluxes. This extraction is required to be done in real-time for the plasma control. Here, we assume that the magnetic fluxes induced by PF coils and eddy currents can be given by the time-delayed signals of PF coil currents. The time-delayed signals are given in the form

$$j_n = (i_n - j_{n-1})\left(1 - \mathrm{Exp}\left[-\frac{\tau_s}{\tau}\right]\right) + j_{n-1}. \quad \cdots\cdots (1)$$

Here, the index of n is time sequence. The i_n and j_n are the raw signal and the time-delayed signal, respectively. The τ_s and τ are the sampling period and the delay time constant, respectively. Usually, the condition of $\tau_s \ll \tau$ is satisfied, the time-delayed signal can be approximated by

$$j_n = (i_n - j_{n-1})\frac{\tau_s}{\tau} + j_{n-1}. \quad \cdots\cdots (2)$$

Figure 2 shows the wave form of PF26 coil current, and the measured flux loop signal. While the measured flux loop signal is not proportional to the PF26 coil current because of the effect of eddy currents, the time-delayed wave with $\tau = 10.4$ msec of PF26 coil current accords well with the measured flux loop signal. Thus, the plasma-induced flux of the k-th flux loop f_k^{meas} is given by

$$f_k^{meas} = \psi_k^{meas} - \sum_c c_{kc}\, j_{kc}, \quad \cdots\cdots (3)$$

as a linear combination of other coils. And, the magnetic flux of the unit plasma current g_k^{meas} is given by

$$g_k^{meas} = f_k^{meas} / I_p^{meas}. \quad \cdots\cdots (4)$$

Here, Ψ_k^{meas} is the measured flux of the k-th flux loop, I_P^{meas} is the measured plasma current, j_{kc} is the c-th coil's time-delayed wave form with time constant τ_{kc}, and τ_{kc} and c_{kc} are the delay time constant and the coefficient of the k-th flux loop and the c-th coil current. The delay time constants and the coefficients are determined on ahead by the least square method. The delay time constant τ_{kc} depends on a pair of the k-th flux loop and the c-th coil, and the determined time constants are over 3 msec and less than 20 msec, which satisfy the condition of $\tau_s \ll \tau$ ($\tau_s = 0.25$ msec, 4 kHz). While this extraction method doesn't consider the effect of eddy currents induced by plasma, the advantage of this method is to be done with light calculation amount, which is appropriate for the real-time calculation. This method has been installed into the main thread of the WS.

2.3 Plasma Position The plasma position can be obtained from the plasma-induced magnetic fluxes with assuming the plasma as one filament current. For this, it is required to calculate the mutual inductance matrix m_{ijk} on ahead. Here, the index of i and j are the mesh number of R and z direction, the k is the k-th flux loop. The calculation procedures are as follows:

(1) Find the mesh point (R_i, z_j) to minimize the error between g_k^{meas} and m_{ijk} of

$$\varepsilon = \sum_k (g_k^{meas} - m_{ijk})^2, \quad \cdots\cdots (5)$$

(2) Make linear approximate functions of the mutual inductances around (R_i, z_j);

$$g_k^{approx} = \frac{m_{i+1,jk} - m_{i-1,jk}}{2\Delta R}(R - R_i) + \frac{m_{i,j+1,k} - m_{i,j-1,k}}{2\Delta z}(z - z_j) + m_{ijk} \quad \cdots\cdots (6)$$

$$\equiv \alpha_k R + \beta_k z + \gamma_k, \quad \cdots\cdots (7)$$

where ΔR and Δz are the mesh sizes of R and z direction,

(3) Solve the simultaneous linear equations about R and z ($\partial\varepsilon/\partial R = 0$, and $\partial\varepsilon/\partial z = 0$) to minimize error of $\varepsilon = \sum_k (g_k^{meas} - g_k^{approx})^2$.

Here, we get the plasma position as

$$\begin{pmatrix} R \\ z \end{pmatrix} = \frac{1}{\boldsymbol{\alpha}^2\boldsymbol{\beta}^2 - (\boldsymbol{\alpha}\cdot\boldsymbol{\beta})^2} \begin{pmatrix} \boldsymbol{\beta}^2 & -\boldsymbol{\alpha}\cdot\boldsymbol{\beta} \\ -\boldsymbol{\alpha}\cdot\boldsymbol{\beta} & \boldsymbol{\alpha}^2 \end{pmatrix} \begin{pmatrix} \boldsymbol{\alpha}^T \\ \boldsymbol{\beta}^T \end{pmatrix} \left(\mathbf{g}^{meas} - \boldsymbol{\gamma} \right). \quad \cdots\cdots (8)$$

To calculate this, the 6 flux loop signals are used (see Fig. 1(b)), and we choose the mesh size as the 50 mm in the range of 250 mm $< R <$ 1250 mm, and -450 mm $< z <$ 450 mm. This calculation method has been installed into the main thread of the WS.

2.4 Plasma Shape In order to represent magnetic fluxes with the plasma shape parameter, we use geometrical center of the plasma (R_0, z_0), current peak axis (R_{ax}, z_{ax}), minor radius a, elongation κ, and triangularity δ as the plasma shape parameters. The magnetic flux g_k^{calc} with these parameters can be obtained with procedures as follows:

(1) Distribute unitary current in a unit circle with parabolic profile,
(2) Represent this current as the collection of filament currents with $[u_m \times u_m]$ mesh grids,
(3) Distribute these filament currents into the vacuum vessel according to the plasma shape parameters,
(4) Calculate the magnetic flux of the k-th flux loop induced by these filament currents with pre-calculated $[v_{mr} \times v_{mz}]$ size mutual inductance matrix m_{ijk}.

In the first and second procedure, the current density is distributed in a unit circle with a profile proportional to $(2/\pi)(1-r^2)$, where $|r| < 1$. This profile is divided into segments with the $[u_m \times u_m]$ mesh grids. Here, we regard one segment as one filament current, and each filament contains information of its position and a current. The summation of all filament currents is unity. In the third procedure, the distribution of the filament currents into the vacuum vessel is described at Appendix A. Now, we can calculate the magnetic fluxes g_k^{calc} as the function of plasma shape parameters

$$g_k^{calc} = g_k^{calc}(R_0, z_0, R_{ax}, z_{ax}, a, \kappa, \delta) . \quad \cdots\cdots (9)$$

In order to calculate the magnetic flux of the k-th flux loop induced by the l-th filament positioned (R_l, z_l) with a current of c_l, there are two ways. One is to use the flux value m_{ijk} of the nearest mesh point (R_i, z_j). The other is to use the flux value m_l calculated by linear interpolation with the usage of near 4 mesh points, where

$$m_l = m_{l0} + (m_{l1} - m_{l0}) \times (z - z_j)/\Delta z , \quad \cdots\cdots (10)$$

and

$$m_{l0} = m_{ijk} + (m_{i+1,jk} - m_{ijk}) \times (R - R_i)/\Delta R , \quad \cdots\cdots (11)$$

$$m_{l1} = m_{i,j+1,k} + (m_{i+1,j+1,k} - m_{i,j+1,k}) \times (R - R_i)/\Delta R . \quad \cdots\cdots (12)$$

In the former case, the mesh size has to be fine for the accurate calculation. On the other hand, it requires less calculation time compared to the latter case.

To save enormous usage of WS memory, the appropriate size of mesh grids $[v_{mr} \times v_{mz}]$ for mutual inductance m_{ijk} has to be determined. We calculate magnetic fluxes of two flux loops placed symmetrically to equatorial plane (R = 198 mm, z = ±550 mm) with the plasma shape parameters symmetrical about the equatorial plane (Fig. 3(a)). The mesh grid area is set to 0.0 m $< R <$ 1.5 m, and -1.5 m $< z <$ 1.5 m. The calculated magnetic fluxes which should be same to each other because of its symmetric property are different, even if the mesh grids is [800 × 1600] (pitch 1.9 mm) without the interpolation. On the other hand, two flux values are almost same with the interpolation. Thus, we choose the mesh grids as [100 × 200] (pitch 15 mm) with the use of the linear interpolation.

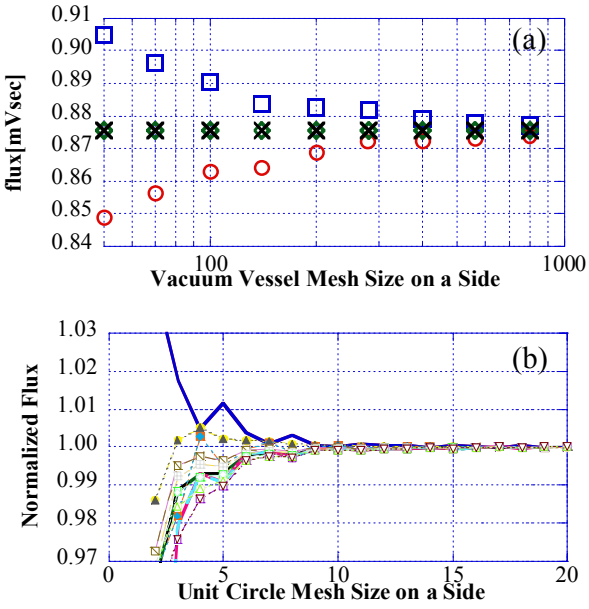

Fig. 3. The calculation accuracy depending on the mesh size: (a) The calculated magnetic fluxes of the two flux loops (FLC7, and FLC18) placed symmetrically to the equatorial plane with the plasma shape parameters symmetrical to the equatorial plane; The fluxes of FLC7 without the interpolation (circle), with interpolation (diamond) and FLC18 without interpolation (square), with interpolation (cross) are shown, (b) The calculated magnetic fluxes of each flux loops normalized by the value of the case of 20 mesh size

The appropriate size of mesh grids for the unit circle has also to be determined. When the mesh grids become large, the calculation accuracy increases, but the calculation time also increases. When the size of mesh grids for the unit circle is set to $[u_m \times u_m]$, the number of filaments to represent the plasma is about $u_m{}^2\pi/4$, which mean that the calculation time increases as the square of the mesh grids u_m. We calculate magnetic fluxes with changing the mesh grids u_m. In the Fig. 3(b), the calculated magnetic fluxes reach to some constant values with the increase of the mesh grids, and the mesh grids u_m should be more than 10 for the calculation accuracy.

Now, it is required to find the plasma shape parameters to minimize the error

$$\varepsilon = \sum_k \left(g_k^{calc}(R_0, z_0, R_{ax}, z_{ax}, a, \kappa, \delta) - g_k^{meas} \right)^2 . \quad \cdots\cdots (13)$$

In Fig. 4, dependence of error value ε on a and κ is shown in one case where g_k^{meas} are set to calculated values with the target plasma shape parameters of $R_0 = R_{ax} = 0.75$ m, $z_0 = z_{ax} = 0.0$ m, $a = 0.4$ m, $\kappa = 1.5$, and $\delta = 0.7$, and plasma shape parameters of g_k^{calc} are same to the target plasma except a and κ. In this figure,

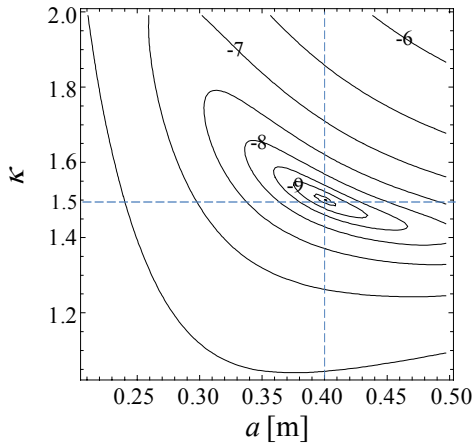

Fig. 4. Contour Plot of $\mathrm{Log}_{10}\varepsilon$ in a-κ plane; Dashed lines denote target parameter values of a and κ

local minimum points do not appear except target shape parameters of $a = 0.4$ m and $\kappa = 1.5$. This reinforces that it is sufficient to find a local minimum point in order to minimize the error function ε.

Since the ranges of parameters to seek are very large, we try to find the appropriate parameters separately. At first, the a, κ, and δ are identified with the assumption that the positions of the geometric center and the current peak axis are same to the plasma position defined previously. After that, these positions are determined. Several iterations between the identification of the plasma shape and the determination of the plasma position may be required. To determine the plasma shape a, κ, and δ, we propose two methods. One is a linear approximation method, and the other one is a downhill simplex method. The procedures of the linear approximation method are as follows:

(1) Set the initial plasma shape parameters a_0, κ_0, and δ_0,

(2) Make the linear approximation functions about a, κ and δ

$$g_k^{approx} = g_k^{calc} + \frac{\partial g_k^{calc}}{\partial a}(a - a_0) + \frac{\partial g_k^{calc}}{\partial \kappa}(\kappa - \kappa_0) + \frac{\partial g_k^{calc}}{\partial \delta}(\delta - \delta_0), \quad \cdots\cdots (14)$$

(3) Solve the simultaneous linear equations about a, κ, and δ ($\partial\varepsilon/\partial a = 0$, $\partial\varepsilon/\partial\kappa = 0$, and $\partial\varepsilon/\partial\delta = 0$) to minimize the error of $\varepsilon = \sum_k (g_k^{approx} - g_k^{meas})^2$.

(4) Check and trim variations of the parameters Δa, $\Delta\kappa$, and $\Delta\delta$, where $\Delta a = a_1 - a_0$, $\Delta\kappa = \kappa_1 - \kappa_2$ and $\Delta\delta = \delta_1 - \delta_2$

The a_1, κ_1 and δ_1 are parameters solved in the third procedure. The absolute values of a_1, κ_1 and δ_1 may have some errors if the initial parameters are unsuitable. Hence, in this procedure, the new parameters are trimmed in order not to exceed the pre-defined permissible variation range, and in order to converge gradually. The new parameters are defined as

$$a = a_0 + \Delta a / t_{\max}, \quad \cdots\cdots (15)$$

$$\kappa = \kappa_0 + \Delta\kappa / t_{\max}, \quad \cdots\cdots (16)$$

$$\text{and} \quad \delta = \delta_0 + \Delta\delta / t_{\max}, \quad \cdots\cdots (17)$$

where

$$t_{\max} = \max\left[\left|\frac{\Delta a}{\Delta a_p}\right|, \left|\frac{\Delta\kappa}{\Delta\kappa_p}\right|, \left|\frac{\Delta\delta}{\Delta\delta_p}\right|\right], \quad \cdots\cdots (18)$$

and the Δa_p, $\Delta\kappa_p$, and $\Delta\delta_p$ are the pre-defined permissible variation ranges.

(5) Iterate from the second procedures in finite times,

(6) Check the last shape parameters.

In the sixth procedure, the converged new parameters are checked whether the plasma is inside of the vacuum vessel or not. If plasma shape intersects with the vacuum vessel wall, the acquired parameters are trimmed in the order of a, κ, then δ. For example, if an inequality $R_{\text{outside}} < R_0 + a$ is satisfied, where R_{outside} is radius of outside wall, this means plasma shape intersects with outside wall, and minor radius a is trimmed to $R_{\text{outside}} - R_0$. If an inequality $z_{\text{topside}} < z_0 + \kappa a$ is satisfied, where z_{topside} is z-position of topside wall, elongation κ is trimmed to $(z_{\text{topside}} - z_0)/a$.

The downhill simplex method[11] is a commonly used technique for minimizing an objective function in a many-dimensional space. This method uses a special polytope of N + 1 vertices in N dimensions, and move the vertices gradually to decrease an objective function. Here, we try to apply this method to minimize the error in the three-dimensional space, a, κ, and δ. The procedures of the downhill simplex method are as follows:

(1) Set the initial N + 1 points (a_i, κ_i, δ_i, i = 1, 2, 3, 4),

(2) Find a new point and replace the old point according to the downhill simplex method,

(3) Check the convergence performance. If not good, resume from the first procedure,

(4) Check the convergence. If not converged, iterate from the second procedure.

In the first procedure, the initial N + 1 points are selected to satisfy linear independence with each other. Namely, we consider three-dimensional space and 4 points as vertices in this case, and these 4 vertices have to be selected in order to compose a tetrahedron. Since each point has components of a, κ, and δ plasma shape can be represented from one point. All the points have to satisfy that plasma shape is inside of the vacuum vessel. In the second procedure, the new point is also checked whether inside of the vacuum vessel. If not, the new point is trimmed in order to be inside. When the linear independence is not satisfied because of this trimming, the initial N + 1 points but differ from the previous one are set in the third procedure. In the fourth procedure, when the difference between N + 1 points become sufficiently small, or the number of iteration exceeds pre-defined value, the calculation is terminated. Whereas the linear approximation method permits the error value to become larger during the iteration, the downhill simplex method doesn't permit during its iteration except for the case that the new initial N + 1 points are set. This can be expected that the downhill simplex method requires much calculation time, but has the high noise immunity.

3. Results

At first, the both methods are tested whether the plasma shape can be found or not under almost all the possible cases of the target plasma shape parameters with the condition of $R_0 = R_{ax}$, and $z_0 = z_{ax}$. The R_0 (= R_{ax}), z_0 (= z_{ax}), and a are scanned by 0.3 m < R_0 < 1.2 m (pitch 0.2 m), −0.5 m < z_0 < 0.5 m (pitch 0.2 m), and 0.2 m < a < 0.45 m (pitch 50 mm), respectively. The κ and δ are scanned by 1.0 < κ < 2.0 (pitch 0.2) and 0.0 < δ < 1.0 (pitch 0.2),

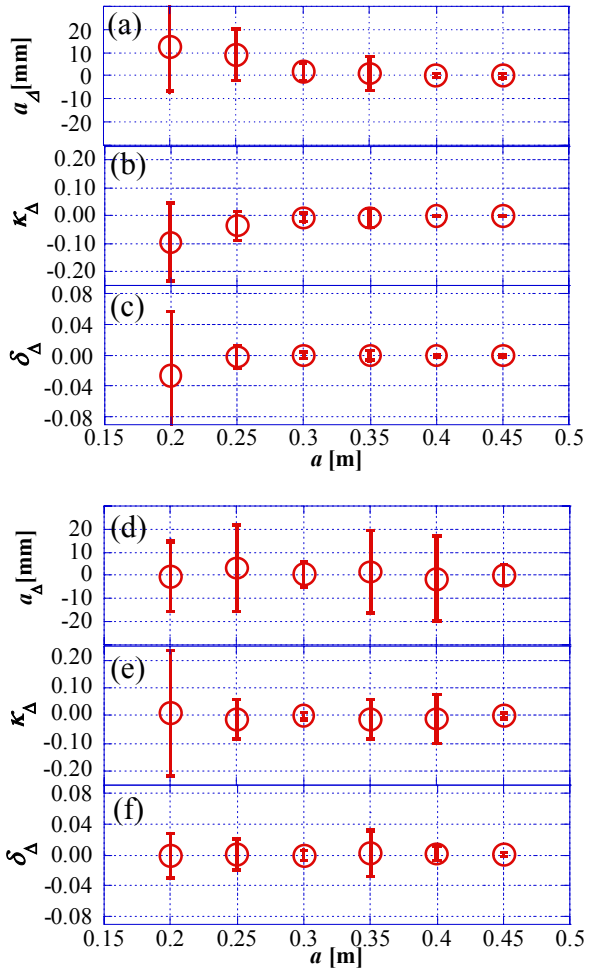

Fig. 5. The reproducibility tests with the linear approximation method (a)-(c), and the downhill simplex method (d)-(f); The a_Δ, κ_Δ, and δ_Δ are the differences between the target plasma shape parameters and the acquired parameters

respectively. The size of unit circle mesh grids on a side is set to 10 in both methods, and the number of iteration is set to 8 in the linear approximation method. Figure 5 shows this result. While the reproducibility of the downhill simplex method is slightly low compared to the linear approximation method, the good reproducibility is obtained in the both methods. In this test, the average number of flux calculation times is 230 with the downhill simplex method.

The calculation times are evaluated in the both methods. The calculation time depends mainly on the size of unit circle mesh grids and the number of iterations in the linear approximation method. In the downhill simplex method, since the number of iterations changes according to its convergence behavior, the calculation time is evaluated as the function of the number of flux calculation. In Fig. 6, the calculation times of the both method are evaluated with the usage of one out of four cores of the controller module of the WS. In the linear approximation method, the calculation time is about 1 msec with 15 mesh grids and 8 times iteration. In the downhill simplex method, the calculation time is about 3 msec with 10 mesh grids and 230 times of flux calculation.

It is important to check the noise immunity of these two methods. The reproducibility is tested under the condition that the

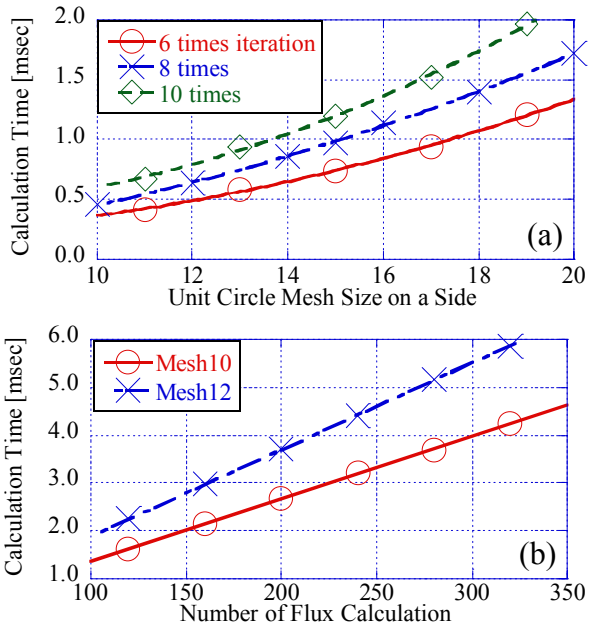

Fig. 6. The calculation time of (a) the linear approximation method, and (b) the downhill simplex method

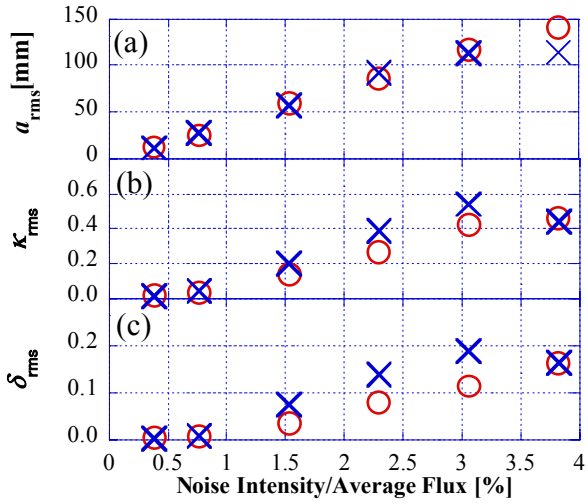

Fig. 7. The noise immunity test of (a) minor radius, (b) elongation, and (c) triangularity for the linear approximation method (circle) and the downhill simplex method (cross); The vertical axes are root mean square (rms) errors between target plasma shape parameters and acquired parameters

random noises are imposed into the target flux,

$$g_k^{\text{target}} = g_k^{calc} + \Delta g r_k , \quad \cdots\cdots (19)$$

where r_k is the k-th random number of $-1 < r_k < 1$. The Δg is same to all the flux loops. The intensity of the imposed noise is evaluated as the ratio of Δg to the averaged flux, $\Delta g / \langle g_k^{calc} \rangle$. The target plasma shape parameters are fixed to $R_0 = R_{ax} = 0.75$ m, $z_0 = z_{ax} = 0.0$ m, $a = 0.4$ m, $\kappa = 1.5$, and $\delta = 0.7$. The dependency of the reproducibility on the imposed nose is shown in Fig. 7. The root mean square (rms) errors are calculated from the 200 test cases. While the error values become large with the increase of noise intensity in both methods, the intensities of errors are not so different in each method. The time evolution of a typical discharge

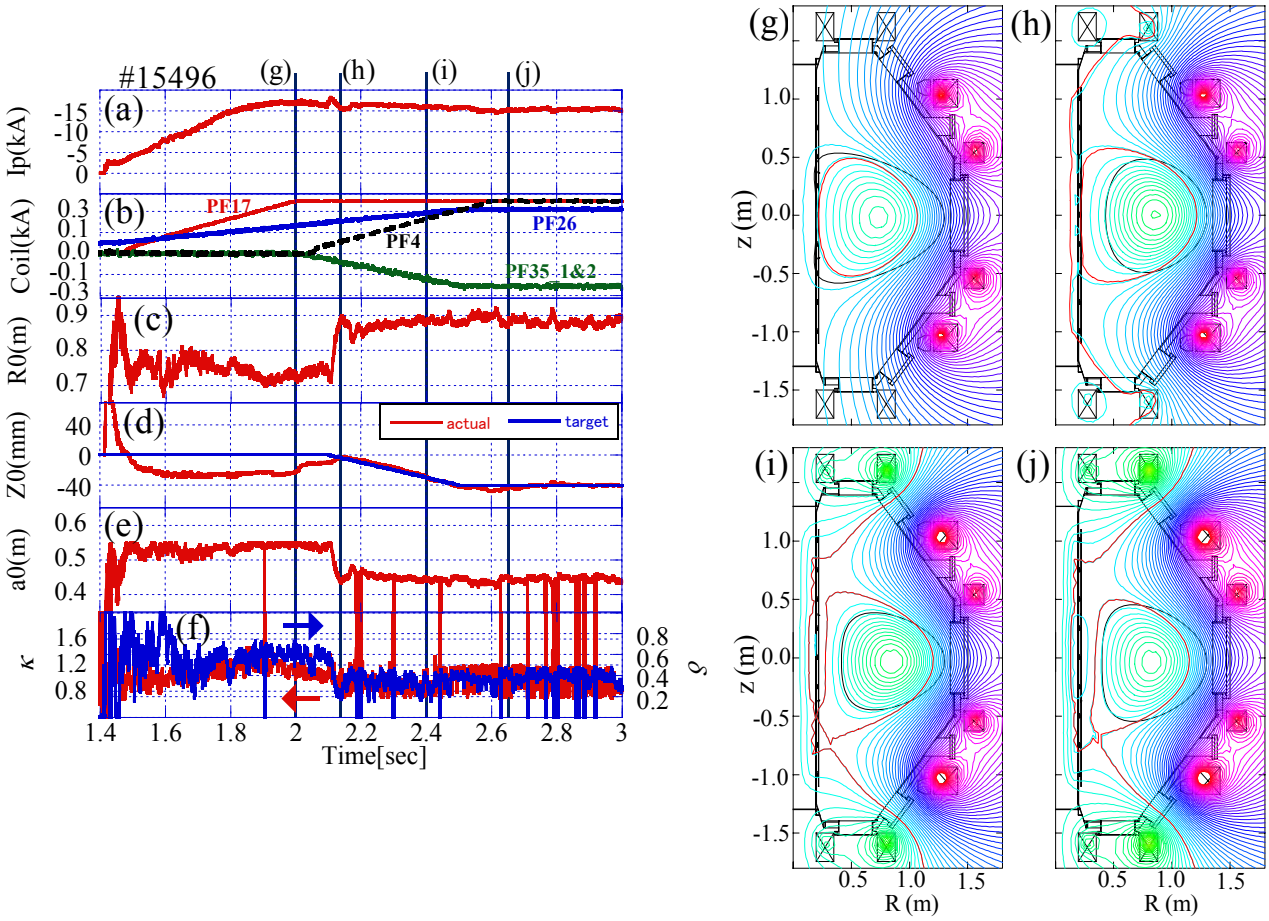

Fig. 8. Time evolution of the divertor discharge: (a) Plasma Current, (b) PF coil currents, (c) Plasma R position, (d) Plasma z position, (e) Minor radius, (f) Elongation and triangularity, (g)-(j) The plasma current shape (black), and the magnetic flux (color) calculated from the coil currents and the plasma current distribution

of 8.2 GHz microwave pulse (90 kW) with B_t = 1.4 kG is shown in Fig. 8. In this discharge, the PF3-1 and PF5-1 (PF35-1) coils, and the PF3-2 and PF5-2 (PF35-2) coils are connected serially, and the PF4-1, PF4-2A, PF4-2B, and PF4-3 (PF4) coils are also connected serially. The time sequence of the coil currents are shown in Fig. 8(b). From the plasma initiation, the PF17 and PF26 coil currents are increased in the positive direction according to the plasma current of the negative direction. The currents of PF35-1 and PF35-2 increase from 2 sec in the same direction to the plasma current, and the current of PF4 also increases from 2 sec in the opposite direction to the plasma current in order to make the divertor configuration. The plasma position calculated by the way described above is shown in Fig. 8(c), and (d). The vertical plasma position is controlled from 2 sec referring this plasma position with PID control installed in the main thread of WS (Fig. 8(d)). The a, κ, and δ calculated by the linear approximation methods are shown in Fig. 8(e), and (f), respectively. In these figures, sudden spike-like signals can be seen as the case that the calculation doesn't converge but vibrates. The found plasma shape and the magnetic fluxes are shown in Fig. 8(g)-(j). The found plasma shape touches vacuum vessel during the discharge in this calculation.

4. Discussions and Summary

Under the assumption of the plasma as one filament current, the plasma position has been calculated in 4 kHz considering the effect of the eddy currents induced by PF coils. The vertical plasma position control is performed referring these values.

To identify the plasma shape, the linear approximation method and the downhill simplex method are tested. The good reproducibility is obtained in both methods, and the calculation times are 1 msec in the linear approximation method and 3 msec in the downhill simplex method with the usage of one out of four cores. Though the downhill simplex method is expected to have high noise immunity compared to the linear approximation method, there is no significant difference between two methods, and the reproducibility is fairly sensitive to the noise intensity in both methods. This may indicate that other local minimums occur in the objective function ε by imposing the slight noise components, and both methods may fail to find the minimum. In order to identify plasma shape parameters appropriately, measured flux values should be determined with satisfactory accuracy compared to averaged flux value. In the case of plasma shape parameters of Fig. 7 and 20 kA plasma current, average of plasma induced fluxes is about 5.2 mVsec. In the WS, flux values are calculated by numerical integration of loop voltage signals which are transferred to FPGA modules of the WS via 1 MHz isolation amplifiers and acquired with 100 kHz sampling frequency. Uncertainties of flux signals may come from insufficient sampling frequency, offset errors of the isolation amplifiers, and quantizing

errors of FPGA modules with resolution of 0.3 mV (±10 V, 16 bits). Since these types of uncertainties are independent of plasma discharge, a signal-to-noise ratio (SNR) can be expected to become high with larger plasma current. Adjustment of voltage gains of isolation amplifiers to suppress quantizing errors is also effective for high SNR. Furthermore, it may be effective to choose the combination of the 22 magnetic flux loops acquired by WS not far from the plasma but near to the plasma in order to increase signal intensities. Since the consistency between obtained plasma shape and results of other measuring instruments has not been verified yet because of the lack of appropriate measuring instruments, its verification should be a future work with using measuring instruments such as soft X-ray array.

While the minimization of the objective function ε including the geometric center (R_0, z_0) and the current peak axis (R_{ax}, z_{ax}) could provide more accurate plasma shape, it would take much time to calculate. For example, suppose that each parameter have 3 candidate values such as R_0, and $R_0 \pm \Delta R_0$, it is required to calculate 81 (= 3^4) times to check all cases of 4 parameters, R_0, R_{ax}, z_0, and z_{ax}. This means that it takes over 100 msec to find appropriate (R_0, z_0) and (R_{ax}, z_{ax}), and this is in the same range to the decay time of the plasma current found in the typical discharges of QUEST. Hence, it is difficult to calculate in real-time including to find (R_0, z_0) and (R_{ax}, z_{ax}).

The new thread to identify plasma shape of a, κ, and δ can be installed into the WS in addition to the already existing two threads because of surplus of the cores. This thread receives the plasma position and 22 plasma-induced magnetic flux signals from the main thread, and can identify the plasma shape with the working frequency of 1 kHz by the linear approximation method. Thus, the identification of the plasma shape parameters can be done within several milliseconds technically under the condition that the geometric center and the current peak axis are same to the plasma position calculated as one filament current. However, it should be kept in mind that the magnetic fluxes have to be measured with high accuracy to use this calculation result for the real-time control.

Acknowledgements

This work is performed with the support and under the auspices of the NIFS Collaboration Research Program (NIFS10KUTR048, NIFS11KUTR059).

References

(1) C. B. Forest, et al. : "Investigation of the formation of a fully pressure-driven tokamak", *Phys. Plasmas*, Vol.1, No.5, pp.1568-1575 (1994)
(2) A. Ejiri, et al. : "Non-inductive plasma current start-up by EC and RF power in the TST-2 spherical tokamak", *Nucl. Fusion*, Vol.49, 065010 (2009)
(3) M. Uchida, et al. : "Start-Up of Spherical Torus by ECH without Central Solenoid in the LATE Device", *J. Plasma Fusion Res.*, Vol.80, No.2, pp.83-84 (2004)
(4) K. Hanada, et al. : "Non-Inductive Start up of QUEST Plasma by RF Power", *Plasma Sci. Technol.*, Vol.13, No.3, pp.307-311 (2011)
(5) J. R. Ferron, et al. : "Real Time Equilibrium Reconstruction for Tokamak Discharge Control", *Nucl. Fusion*, Vol.38, pp.1055-1066 (1988)
(6) D. A. Gates, et al. : "Plasma shape control on the National Spherical Torus Experiment (NSTX) using real-time equilibrium reconstruction", *Nucl. Fusion*, Vol.46, pp.17-23 (2006)
(7) H. Wang, J. Luo, and Q. Huang : "Real Time Equilibrium Reconstruction Algorithm in EAST Tokamak", *Plasma Sci. Technol.*, Vol.6, No.4, pp.2390-2394 (2004)
(8) A. Ejiri, et al. : "RF start-up and sustainment experiments on the TST-2@K spherical tokamak", *Nucl. Fusion*, Vol.46, pp.709-713 (2006)
(9) Y. S. Hwang, C. B. Forest, D. S. Darrow, G. Greene, and M. Ono : "Reconstruction of current density distributions in the CDX-U tokamak", *Rev. Sci. Instrum.*, Vol.63, No.10, pp.4747-4749 (1992)
(10) T. Yoshinaga, M. Uchida, H. Tanaka, and T. Maekawa : "A current profile model for magnetic analysis of the start-up phase of toroidal plasmas driven by electron cyclotron heating and current drive", *Nucl. Fusion*, Vol.47, pp.210-216 (2007)
(11) J. A. Nelder and R. Mead : "A simplex method for function minimization", *Computer Journal*, Vol.7, pp.308-313 (1965)

Appendix

1. Procedure to Distribute the Filaments into the Vacuum Vessel

The distribution of the filament currents into the vacuum vessel according to the plasma shape parameters is obtained with the procedures as follows:

(1) Displace the filament positions according to the R_{ax}, z_{ax},

$$\vec{r}_{l1} = \vec{r}_{l0} + \left(1 - |\vec{r}_{l0}|^2\right)\begin{pmatrix} (R_{ax} - R_0)/a \\ (z_{ax} - z_0)/(\kappa a) \end{pmatrix}, \quad \cdots\cdots (A1)$$

where $\vec{r}_{l0}$ is the initial position of the l-th filament in a unit circle of x-y plane, and $\vec{r}_{l1}$ is the new position. While the filaments on the unit circle ($|\vec{r}_{l0}| = 1$) don't move, the filament on the center of the unit circle ($|\vec{r}_{l0}| = 0$) moves to $((R_{ax} - R_0)/a, (z_{ax} - z_0)/(\kappa a))$. All the filaments remain inside of the unit circle.

(2) Multiply the filament positions by a and κa in x-direction and y-direction, respectively,

$$\vec{r}_{l2} = \begin{pmatrix} a & 0 \\ 0 & \kappa a \end{pmatrix}\vec{r}_{l1}. \quad \cdots\cdots (A2)$$

The unit circle become the ellipse with the x-axis of a, and the y-axis of κa.

(3) Displace the filament positions in x-direction according to the δ,

$$\vec{r}_{l3} = \begin{pmatrix} r_{l2x} - \dfrac{\delta a}{(\kappa a)^2} r_{l2y}^{\,2} \\ r_{l2y} \end{pmatrix}. \quad \cdots\cdots (A3)$$

The filament positioned on the top of ellipse (r_{l2x}, r_{l2y}) = (0, κa) moves to the new position (r_{l3x}, r_{l3y}) = ($-\delta a$, κa).

(4) Move the filament into the vacuum vessel according to the R_0, z_0,

$$\vec{r}_{l4} = \vec{r}_{l3} + \begin{pmatrix} R_0 \\ z_0 \end{pmatrix}. \quad \cdots\cdots (A4)$$

Makoto Hasegawa  (Non-member) received his B.Sci., and M.Sci. from Faculty of Science, Kyoto University in Japan in 1995, and School of Science, Tokyo University in 1997, respectively. He became a research associate of Kyushu University in Fukuoka, Japan in 2000, and received his D.Eng. from Interdisciplinary Graduate School of Engineering Sciences, Kyushu University. His main research interests are systems of data acquisition, remote experiment participation, WEB-based techniques, and plasma equilibrium and its control. He is a member of the Physical Society of Japan (JPS), and the Japan Society of Plasma Science and Nuclear Fusion Research (JSPF).

Kazuo Nakamura  (Member) received his B.Eng., M.Eng. and D.Eng. from Department of Electrical and Electronic Engineering, Nagoya University in Aichi, Japan in 1974, 1976 and 1983, respectively. He became a research associate, an associate professor and a full professor of Kyushu University in Fukuoka, Japan in 1977, 1984 and 1997, respectively. His main research interests include power plant, power supply, power electronics, plasma equilibrium, plasma control, plasma heating and current drive, plasma surface interaction and plasma diagnostics. He is a member of the Institute of Electrical Engineers of Japan (IEEJ), the Physical Society of Japan (JPS), and the Japan Society of Plasma Science and Nuclear Fusion Research (JSPF).

Kazutoshi Tokunaga  (Non-member) received his B.Sci. from Faculty of Science, Kumamoto University in Japan in 1984. He also received M. Eng. and D. Eng. from Interdisciplinary Graduate School of Engineering Sciences, Kyushu University in Japan in 1987 and 1993, respectively. He became a research associate and an associate professor of Kyushu University in Fukuoka, Japan in 1990 and 1997, respectively. His main research interests are plasma wall interactions, radiation damage of the first wall/divertor materials and development of the high heat flux components in fusion devices. He is a member of the Atomic Energy Society of Japan (AESJ), the Japan Society of Applied Physics (JSPA), and the Japan Society of Plasma Science and Nuclear Fusion Research (JSPF).

Hideki Zushi 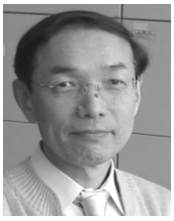 (Non-member) received his D. Eng. from Department of Nuclear Engineering, Kyoto University. He is a full professor at the Advanced Fusion Research Center at the Research Institute for Applied Mechanics, Kyushu University. His research interests include science and engineering of plasma diagnostics, and confinement plasma. He is a member of the Physical Society of Japan (JPS), and the Japan Society of Plasma Science and Nuclear Fusion Research (JSPF).

Kazuaki Hanada  (Member) received his B.Sci., M.Sci, and D.Sci. from Department of Science, Kyoto University in Kyoto, Japan in 1987, 1989, and 1994, respectively. He became an engineering official on Kyoto University in Kyoto, Japan, and a research associate of University of Tokyo in Tokyo, Japan, and an associate professor, and a full professor of Kyushu University, Fukuoka, Japan in 1990, 1994, 1997, and 2001, respectively. His main research interests include plasma heating, current drive, plasma surface interaction and plasma diagnostics. He is a member of the Physical Society of Japan (JPS), and Institute of Electrical Engineers of Japan (IEEJ), and the Japan Society of Plasma Science and Nuclear Fusion Research (JSPF).

Akihide Fujisawa 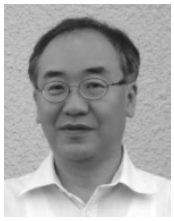 (Non-member) received his B.Eng., M.Eng. and D.Eng. from Department of Electrical and Electronic Engineering, University of Tokyo, Japan in 1985, 1987 and 1990, respectively. He was employed as a research associate in National Institute for Fusion Science (NIFS), 1990, and was promoted to an associate professor there 1998. He moved to Kyushu University as a full professor, 2009. The major research subjects of his are plasma turbulence experiments, nonlinear dynamics of magnetized confinement plasmas. He is a member of the Physical Society of Japan (JPS), and the Japan Society of Plasma Science and Nuclear Fusion Research (JSPF).

Hiroshi Idei  (Non-member) received the B.S. degree in physics from the Shizuoka University, Japan in 1988, the M.S. and the Ph.D degrees in physics from the Nagoya University, Japan in 1990 and 1995. From 1993 to 2003, he was a Research Associate at the Plasma Heating Division at the National Institute for Fusion Science. Since 2003, he has served as an Associate Professor at the Advanced Fusion Research Center at the Research Institute for Applied Mechanics, Kyushu University. His research interests include plasma confinement research, plasma heating/current drive using micro- and millimeter-waves, plasma diagnostics using micro- and millimeter-waves, and micro- and millimeter-wave components.

Shoji Kawasaki  (Non-member) graduated from Electrical Department of Amakusa Technical High School. He is a staff of Technical Services Division of Research Institute for Applied Mechanics, Kyushu University. He engages in specialized and technical occupations including electric and electronic circuits.

Hisatoshi Nakashima 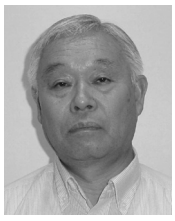 (Non-member) graduated from Kumamoto Technical High School. He is a technical staff of Research Institute for Applied Mechanics, Kyushu University. He is actively engaged in maintenance and safety management of vacuum pumping and water cooling systems.

Aki Higashijima  (Non-member) received a bachelor's degree in biochemical system engineering from Kyushu Institute of Technology. After two years of working as SE in the private company, she works as a technical service staff at RIAM, Kyushu University. She supports data acquisition, control system, and network service.